Fixed-Bed Column Adsorption of PFOA and PFOS from Aqueous Solution Using Maize Tassel Pellets

Pinky Mokwena, OJ Okonkwo[*],

Department of Environmental, Water and Earth Sciences, Tshwane University of Technology, South Africa

ABSTRACT

This study was conducted with the primary aim of assessing the efficiency and practicality of the adsorption of PFOA and PFOS onto fixed-bed column through maize tassel pellets. The effects of bed height (0.5 g -1.5 g), flow rate (0.5 L min^{-1}-2.5 L min^{-1} x 10^{-3}L min^{-1}) and initial concentration (5 mg L^{-1}-20 mg L^{-1}) were investigated and three models were employed to evaluate the performance of the adsorption experiment. The Thomas, Adams-Bohart and Yoon-Nelson models were selected for this purpose. The adsorption rate constants and their respective correlation coefficients were also determined. It was found that an increase in initial concentration of both PFOA and PFOS from 5 mg L^{-1} to 20 mg L^{-1} resulted in higher uptakes at average bed loading. Additionally, it was noted that an increase in bed height for adsorption had a threshold for highest uptake with increase from 0.5 g to 1 g showing an increase in removal. However, desorption pattern was observed when bed height was increased from 1 g to 1.5 g. The removal of both PFOA and PFOS fitted Thomas model, but did not conform satisfactorily to the Adams-Bohart and Yoon-Nelson. It was also observed that there was an increase in K$_{TH}$ values from 7.311 L min^{-1} mg x 10^{4} L min^{-1} mg to 7.532 L min^{-1} mg x 10^{4} L min^{-1} mg and 6.831 L min^{-1} mg x 10^{4} L min^{-1} mg and 7.722 L min^{-1} mg x 10^{4} L min^{-1} mg for PFOA and PFOS respectively as the flow rate increased from 0.5 10^{-3}L min^{-1} to 1.5 10^{-3} L min^{-1}. Moreover, the behaviour of MT pellets for the removal of PFOA and PFOS from surface water indicated that the adsorption was based on a high driving force that was influenced by the increase in initial PFASs concentration. The concentrations of PFOA and PFOS prior to all treatment were calculated at 195 ng mL^{-1} and 120 ng mL^{-1} respectively after the SPE extraction and LCMSMS analysis, and the column study treatment resulted in final concentrations of 31.25 ng mL^{-1} and 29.4 ng mL^{-1} for PFOA and PFOS respectively after removal, which is indicative of a 83.9 % removal of PFOA and more than 75.5 % of PFOS removal.

Keywords: Fixed-bed column; Maize tassel pellets; PFOA/PFOS removal; Aqueous medium

INTRODUCTION

The cumulative growth and development of any society thrives, among others, on the quality of its water. When water quality is compromised as a result of pollution, innovative solutions ought to be developed to aid in the challenge. The class of organic chemicals known as per or polyfluoroalkyl substances (PFASs) have gained a wide interest among researchers on account of their presence in groundwater [1], surface water [2], and other water matrices [3,4]) globally. These compounds are often introduced into the environment when their product carriers such as food packaging containers [5], insecticides [6], furniture coatings [7], fire-fighting film foams [8], and grease resistant cookware [9], are indiscriminately discarded and they seep into water matrices. Their tendency to bioaccumulate without ever breaking down amplifies their effects on water quality, and the strength of their C-F bond [10] makes them impossible to remove from water systems using conventional treatment techniques. These organic chemicals have toxic implications on the health of humans and animals such as cancer and birth dysfunctionalities in humans when water contaminated with these chemicals are consumed. As a result, the removal of these PFASs in water is very important, particularly because of their rising concentration above the standards determined by [11] and the Stockholm Convention on Persistent Organic Pollutants

The current well known removal treatments for pollutants as complex as PFASs includes the use of ion exchange resins, chemical precipitation, magnetic nanoparticles, nano filtration, reverse osmosis, and adsorption techniques [12-14]. As many as these treatment options may exist, most of them have significant drawbacks such as high cost of operation and the need for large storage facilities, i.e., chemical precipitation, and the need for additional treatment options. As a result, sustainability and other studies have reported adsorption as one of the most viable options. Adsorption technique, in acute contrast to others, is highly economical, and

has the capacity to remove these contaminants even at trace levels. This ability is due to the active sites of some materials to attract ionic/functional groups of pollutants. Adsorption techniques for water and wastewater treatment purposes due to its simplicity, low cost of operation and wide use have been reported [15-19].

Adsorbents of biological origin, including alginate, dead and living biomasses, chitosan, lignin and others have been utilized in removing contaminants from water [20]. The efficiency of maize tassel (MT) powder to remove toxic pollutants from aqueous solutions has been widely reported [18–20]. Maize tassel occurs on the male flower that grows at the apex of the maize stalk. Maize tassel is a waste biomaterial that is disposed by farmers after the maize cobs have been harvested [20]. The use of raw maize tassel, as a form of agricultural waste introduces a cutting edge technique that will make the removal of PFASs a practice that is accessible to all.

In this study, the efficiency and practicality of the adsorption of PFOA and PFOS onto fixed bed column through maize tassel pellets were investigated. The effects of bed height (0.5 g^1.5 g), flow rate (0.5 L min^{-1}-2.5 L min^{-1} x 10^{-3}L min^{-1}) and initial concentration (5 mg L^{-1}-20 mg L^{-1}) were investigated and three models were employed to evaluate the performance of the adsorption performance. The Thomas, Adams-Bohart and Yoon-Nelson models were selected for that purpose, and the adsorption rate constants as well as their respective correlation coefficients were also determined.

MATERIALS AND METHODS

The reagents and analytical standards used in the present study included: Methanol–LCMSMS grade, Sigma Aldrich, Germany), ultrapure water was supplied by Separations, South Africa as developed by Siemens, Germany. The acetic acid, hydrochloric acid, glutaraldehyde and ammonium acetate that were used were also purchased from Sigma Aldrich (Pty) Ltd. PFASs standards used in this study are listed below, and they were similarly purchased from Wellington Laboratories (Guelph, Ontario, Canada) in volumes of 1.20 mL and concentrations of 50 mg L^{-1} (Table 1).

All solvents used were of analytical grade and were of high quality

Table 1: List of standards used in this study

Code	IUPAC Name	Mol wt (g/mol)	No of Fluorine atoms
PFOA	2,2,3,3,4,5,5,6,6,7,7,8,8,8- Perfluorooctanoic acid	414.07	15
PFOS	1,1,2,2,3,3,4,4,5,5,6,6,7,7,8,8,8-Heptadecafluorooctane-1-sulfonic acid	500.13	17
MPFOA	Perfluoro-n-[1,2,3,4,13C4]octanoic acid	422	15

Preparation of adsorbent powder

From a maize farm located in Brits, North West Province, South Africa, maize tassels were collected at random, placed into polythene containers and air dried for two weeks. These flowers were harvested based on availability and abundance during the harvest season, and their specific cultivar is Variety Mode 1114. The dried maize tassels were washed, dried and ground into fine powder using a hammer mill (Roff C-80).

Preparation of MT pellets

From the powdered form of the harvested maize tassel, 50 % was then prepared into pellets of average mass of 0.027 g. About 8 g of MT powder was added to 50 mL of ultrapure water in a beaker and stirred together until a greenish brown pasty mixture was formed. In addition to this, 60 µL of acetic acid were added to the mixture, and sonicated for 10 min before 5 mL of glutaraldehyde was pipetted into the now thick slurry solution. These were then sonicated for 15 min, transferred into baking trays and left to bind for 24 h at 50°C. For each 8 g powder sample, 192 pellets were drawn.

Surface water extraction

Four water samples were prepared per compound, namely, one 500 mL blank, two (500 mL) recovery samples as well as a 500 mL surface water sample. Before extraction, the blank, surface water and the recovery (ultrapure) samples were spiked with 25 µL of mass labeled standards of 50 ng mL^{-1} concentration PFOA and PFOS surrogate standards and allowed to equilibrate for 2 h. The internal standard was additionally spiked into the surface water sample (25 µL-50 ng mL^{-1}). The often mandatory step of filtration of the surface water sample was not performed, as it has the potential to result in analyte losses due to the surfactant features of the PFASs [21-24]; therefore, the samples were spiked and analyzed as they were originally obtained from the river.

For SPE extraction, 200 mg per 6 mL HLB cartridges were used. The cartridges were conditioned with 5 mL MeOH followed by 5 mL deionized water. The samples were then loaded onto the pre-conditioned cartridges at a monitored flow rate of 3 mL min^{-1}-6 mL min^{-1} under moderated vacuum conditions. The cartridges were dried for 35 min under vacuum after extraction, and then washed and eluted with 5 mL MeOH twice (10 mL MeOH in total). The eluted extracts were then dried to incipient dryness under a gentle stream of nitrogen gas. They were then reconstituted with 50 µL of MeOH and 50 µL of each surrogate of 50 µg mL^{-1}. The final volume before injection into the LC-MS/MS was 1 mL for each of the samples, and each vial was additionally spiked with 10 µL of the internal standard (MPFOA) for the analysis.

Column experiments

Fixed bed column studies were investigated using a glass column of Internal Diameters (I.D) of 25 mm and 40 cm in length. Maize tassel pellets were packed in column supported by glass wool and inert glass beads at the bottom and top ends following the bottom top direction of flow (Figure 1). Spiked ultrapure water was introduced into the column using a Watson Marlow-101U/R peristaltic pump in the up flow mode to ensure the complete wetting of the beads in the column. All experiments were conducted at room temperature,

25°C and a predetermined pH of 2.0. The columns were packed with noted amount of adsorbent which was sandwiched between two outer layers of glass beads of 3.0 mm diameter and glass wool. The outer ends material packed in column setup were added to dampen the pressure, preventing the pack up of adsorbent on one end against another.
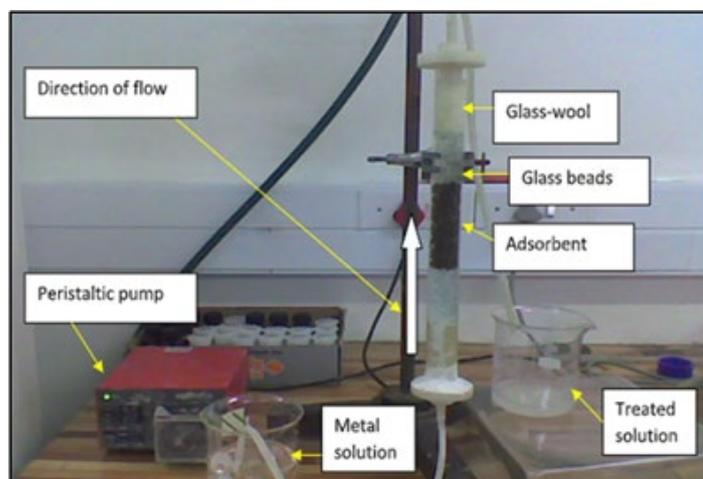
Figure 1: Experimental set-up of the fixed bed adsorption column studies

The effects of bed loading, initial concentration and volumetric flow rate were investigated. The samples were taken at known time intervals starting from 30 min until equilibrium was reached. Parameters tested and their conditions are shown in Table 2. The residual PFAS concentrations in the solution (collected samples) were then analyzed using the same LC-MS/MS 8030 Table 2

Table 2: Experimental conditions for column runs

Column No	Adsorbent height in column (cm)	Column ID (mm)	pH	Flow rate(x 10^{-3} L min^{-1}	Feed concentration (mg L^{-1})
1	0.5	25	2	2.5	5
2	1	25	2	2.5	5
3	1.5	25	2	2.5	5
4	1	25	2	0.5	5
5	1	25	2	1.5	5
6	1	25	2	2.5	5
7	1	25	2	2.5	5
8	1	25	2	2.5	5
9	1	25	2	2.5	10
10	1	25	2	2.5	20

Kinetic models

Three models, namely the Thomas, Adam-Bohart and Yoon-Nelson were used for kinetic studies [25-27]. The Thomas model records the maximum solid phase concentrations of PFAS on pellets, the rate of adsorption constant as well as the maximum adsorption capacity of the adsorbent needed [25]. It is generally employed to evaluate column performance theory, as expressed by:

$$\frac{C_t}{C_o} = \frac{1}{1 + \exp\left[K_{Th}\left(\frac{q_{Th}^m}{Q}C_o t\right)\right]}$$

where, Ct is the effluent concentration at time t (mg L^{-1}), Co is the inlet concentration (mg L^{-1}), Q the flow rate (x 10^{-3}L min^{-1}), m the mass of the adsorbent in the column (g), t the time (min), and K_{TH} the kinetic rate constant for the Thomas model (x 10^{-3}L min^{-1} mg^{-1}) and qTh the maximum adsorption capacity (mg g^{-1}).

The Adam-Bohart model is mainly used for the description of the initial part of the break through curve, as it assumes that the adsorption rate is proportional to both the residual capacity of the adsorbent and the concentration of the adsorbing species [26]. This model can be expressed as follows:

$$In\left(\frac{C_t}{C_o}\right) = k_{BA}C_o t - k_{BA}N_o\left(\frac{z}{U_o}\right)$$

where kBA (x 10^{-4} L mg^{-1} min) is the kinetic constant, N$_o$ (mg L^{-1}) is the saturation concentration, z (cm) is the adsorbent bed depth and U$_o$ (cm min^{-1}) is the linear velocity defined as the ratio of volumetric flow rate (x 10^{-3}L min^{-1}) to the cross sectional area (cm^2) of the bed. These values can be computed from the break through curve of C$_t$/C$_o$ of the above non-linear expression versus t at a chosen bed height and flow rate.

The Yoon-Nelson is a simpler model in comparison to the previous two. Yoon and Nelson model is developed for a single component system, whose parameters-A represents a fraction of the solute adsorbed in bed and P representing the fraction of the solute that remains in an effluent after the adsorption process is concluded [27].

According to this model, the rate of adsorption is expressed as:

$$\frac{-dA}{dt} = k_{YN}.(t - r)$$

Where, k$_{YN}$ is the rate constant (h^{-1}). From the linear dependence of ln [c/(c$_o$-c)] versus time t, the model parameters mentioned in equation above can be determined for any given bed depth, flow rate and initial concentration

## RESULTS AND DISCUSSION

Maize tassel pellets

The pellets formed from the immobilization of powdered maize tassel in glutaraldehyde and acetic acid was reasonably circular in shape, and their diameters were in the range of 2.48 mm ± 0.54 mm.

The effect of bed heights and time on PFOA/PFOS adsorption by maize tassel pellets

As can be seen in Figure 2, the Time (t) which defines the break through time, and exhaustion time are directly proportional to bed height, in that as loading was increased, so too did time (t). In light of this, the plot shapes and gradients obtained were as expected, as it relates to the dynamic adsorption studies of [27]. The increase

in bed height from 0.5 g to 1 g yielded a higher uptake in PFASs with adequate time for both PFOA and PFOS. At bed height of 1 g, a steady and consistent higher uptake can be noted from the first 100 min of experiment in both graphs, and this increase is noted even up till 350 min. However, at both 0.5 g and 1.5 g, uptakes decreased with time. This phenomenon may be a function of the adsorbent availability of active binding sites for the process, which are enhanced by time in that the adsorptive surface can be covered on a more expanded basis. Additionally, it can be noted in Figure 2a that PFOA adsorption reached equilibrium at faster rates than PFOS Figure 2b. According to the study by [28], an increase in bed height at adequate adsorption times is often a precursor to an increase in the mass transfer zone, which directs movement from the entrance of the bed towards its exit for both plots (Figures 2a and 2b).

The effect of influent flow rate on PFOA/PFOS adsorption by maize tassel pellets
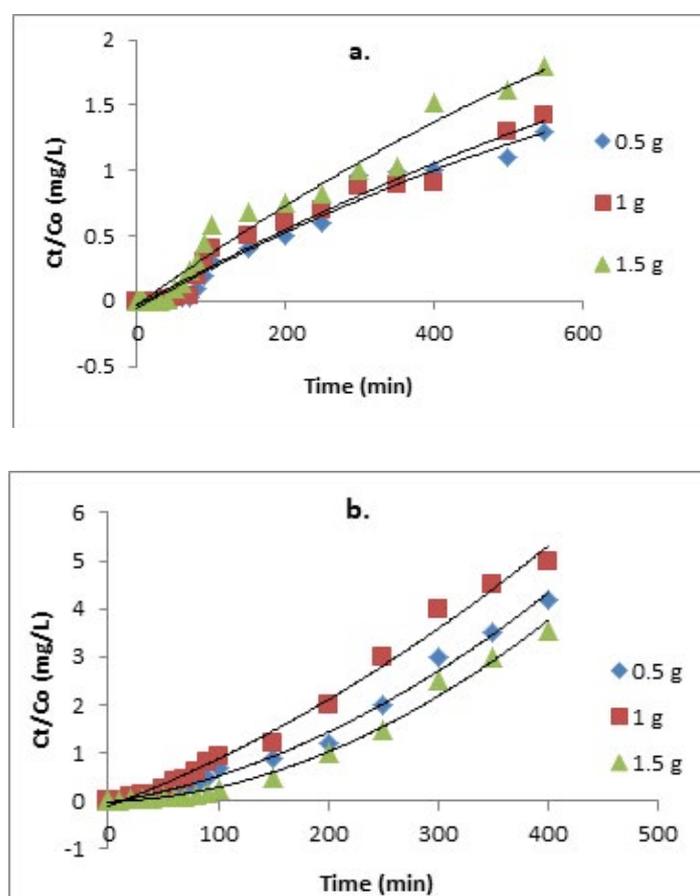
Figure 2: Effect of bed loading of maize tassel pellets and time onto (a) PFOA and (b) PFOS (Initial conc. 5 mg L^{-1}, flow rate 2.5 x 10^{-3}L min^{-1}, column diameter 25 mm)

The effect of flow rate was investigated through variations of 0.5 L min^{-1}, 1.5 L min^{-1} and 2.5 L min^{-1} x 10^{-3}L min^{-1} with fixed levels of bed loading at 1 g and initial PFASs concentrations at 5 mg L^{-1}. The results are illustrated in Figures 3a and 3b respectively. The plots show that at a higher flow rate, the initial point of interaction between the adsorbent and adsorbate display a quick column saturation process in the first 100 min of experiment, which denotes a shorter contact time before the adsorption process takes place. On the other hand, at slower flow rates, longer contact times were needed and the adsorption process displayed a shallow curve

(both Figures 3a and 3b).
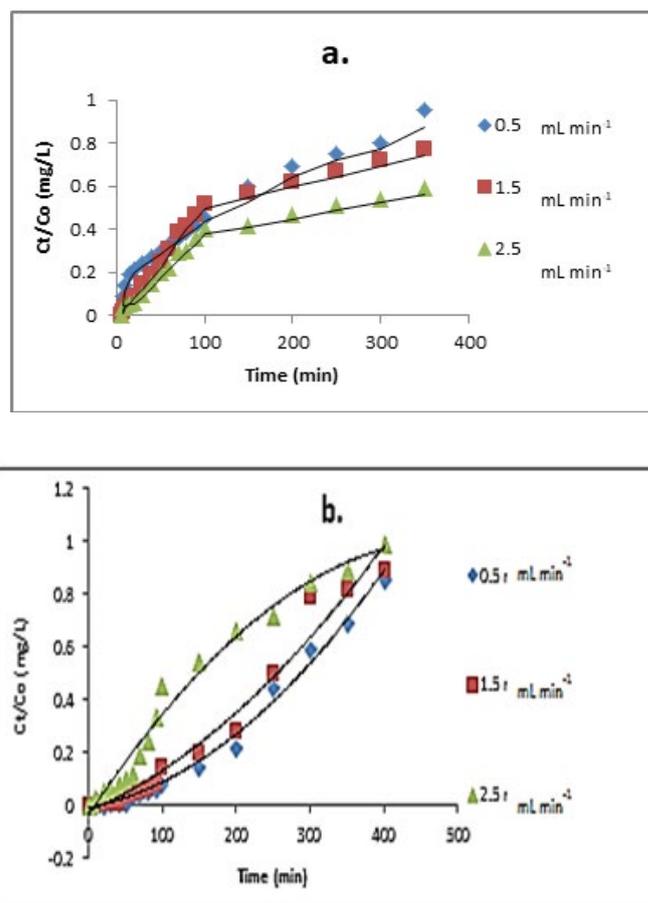
Figure 3: Effect of volumetric flow rate of maize tassel pellets onto (a) PFOA and (b) PFOS)-initial concentration 5 mg L^{-1}, bed loading of 1g and a column diameter of 25 mm.

Moreover, the present study concurs with that by [29], in that exhaustion rate was shown to be a relative influence of adsorption capacities, and the speed with which adsorption takes place is a significant function of the feasibility of the performance of any sorptive material.

Effect of adsorbate concentration

The effects of adsorbate, PFOA/PFOS on the column performance was studied by varying the inlet concentrations of 5, 10 and 20 mg L^{-1}, while the bed loading and flow rate were kept constant at 1 g and 2.5 L min^{-1} x 10^{-3}L min^{-1} respectively. The break through curves for both PFOA and PFOS are illustrated in Figures 4a and 4b respectively. From the plots, it can be easily noted how the MT pellets were exhausted faster (within the first 100 min at higher PFAS inlet concentrations, that is mg L^{-1}, as opposed to the uptake levels of the lower concentrations (which only occurred closer to the 100 min mark). This denotes that the earliest break through point between the three curves was reached when the initial concentrations were higher. This observation may be because lower gradients resulted in slower transportation/movement due to a decrease in the diffusion or mass transfer coefficients. Similar observation was also noted in a study by [30]. Therefore, it can be assumed that the speed at which adsorptive performance occurs depends on the quantities of analyte concentration in a column system.
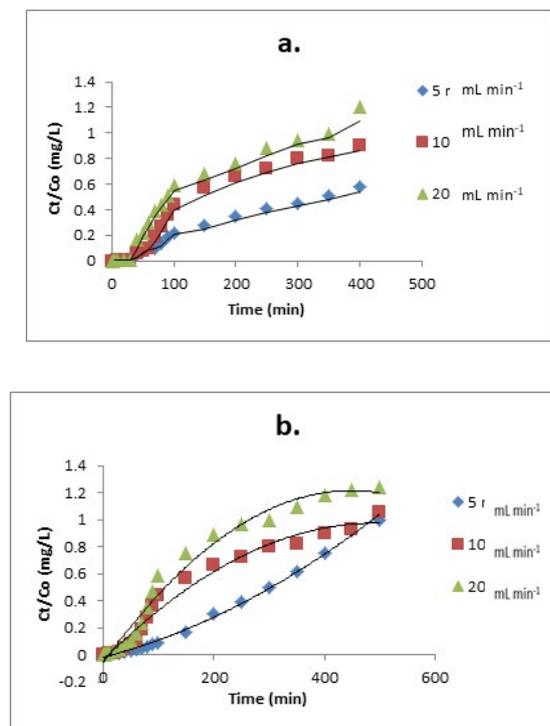
Figure 4: Effect of initial concentration on (a) PFOA and (b) PFOS on adsorption via maize tassel pellets with a bed loading of 1 g and column diameter of 25 mm)

Application of dynamic adsorption model parameters to surface water

The effect of maize tassel pellets in surface water obtained from the Appies River was also investigated. The experiment was done with the aim of targeting PFOA and PFOS in the surface water sample based on the objective of testing the feasibility of the model determined via this study on the efficiency of MT in removing these target PFASs in actual water. The water was obtained at the centre of the Appies River in Pretoria, South Africa.

The water sample was subjected to the same conditions as described in earlier sections of this study. The dynamic adsorption results as can be seen in Figure 5 indicate that the adsorption capacity increased from 70% removal to 79% and 68% to 77.54% for PFOA and PFOS respectively after the inlet concentration was increased to 20 mg L^{-1} during fixed bed column studies at break through points. The concentrations of PFOA and PFOS prior to all treatment were calculated at 98 ng mL^{-1} and 125 ng mL^{-1} respectively after the SPE extraction and LCMSMS analysis, and the column study treatment

resulted in final concentrations of 29.4 ng mL^{-1} and 31.25 ng mL^{-1} for PFOA and PFOS respectively after removal. This observation is a form of reiteration of the results obtained in batch studies, in that when the concentrations of both PFOA and PFOS was spiked into surface water at 20 mg L^{-1}, the removal percentage increased by approximately 10% for both experiments after being spiked with an additional volume of PFASs. These results concur with [31] study that reported that at increased initial concentrations, any adsorption process has a higher driving force. This phenomenon is credited to the fact that more adsorption sites are covered by the pellets in these conditions, especially at the established pH and temperature conditions for removal as detailed in our batch study.
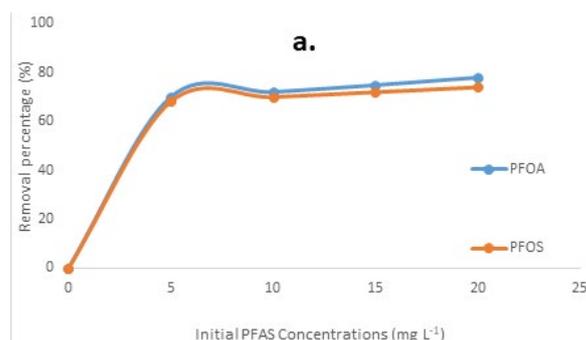
Figure 5: PFOA and PFOS adsorption from surface water using maize tassel pellets

Thomas model

The fixed bed data obtained from adsorption experiment of PFAS in aqueous media was fitted to the Thomas model in order to define the Kinetic Rate Constant (K_{TH}) and maximum adsorption capacity (q_o). The correlation coefficient (R^2) was determined using linear regression. Table 3 shows that there is a decrease in K_{TH} values with an increase in bed loading, which connotes an increase in mass transport resistance for both PFOA and PFOS. It can additionally be observed that there was an increase in K_{TH} values from 7.311 L min^{-1} mg x 10^4 L min^{-1} mg to 7.532 L min^{-1} mg x 10^4 L min^{-1} mg and 6.831 x 10^{-1} and 7.722 L min^{-1} mg x 10^4 L min^{-1} mg for PFOA and PFOS respectively as the flow rate increases from 0.5 L min^{-1} x 10^{-3} L min^{-1} to 1.5 x 10^3 L min^{-1}. The results in Table 3 showed position points that suggest that the Thomas model gave a good description of PFOA and PFOS adsorption onto MT pellets with an average correlation factor of 0.910. This is in relation to the assumption that the sorption of PFASs are not only limited to the chemical interactions with MT pellets but also by the mass transfer at the interface, and was satisfactorily fitted with results by [32] study.

Table 3: Dynamic adsorption parameters for PFOA/PFOS removal by MT pellets – Thomas model

	K_{TH} (x10^{-3} L min^{-1} mg)		Qo (mg L^{-1})		R^2	
	PFOA	PFOS	PFOA	PFOS	PFOA	PFOS
Bed loading (g)						
0.5	0.788	0.683	61.37	25	0.908	0.841
1	0.802	0.861	29.4	12.5	0.930	0.860

1.5	0.224	0.817	5.3	8.333	0.969	0.930
Flow ware (x10^{-3} L min^{-1})						
0.5	0.731	0.750	4.658	4.837	0.547	0.935
1.5	0.753	0.772	14.134	14.108	0.679	0.948
2.5	0.731	0.616	24.647	22.254	0.653	0.850
Initial concentration (mg L^{-1})						
5	0.746	0.719	24.294	24.864	0.843	0.947
10	0.394	0.329	49.157	51.218	0.842	0.872
20	0.177	0.154	105.914	110977	0.785	0.851

Adam-Bohart model

In order to describe the initial parts of the break through curves, this model was applied to the experimental data. The estimated parameters, such as the kinetic constant (K_{AB}) and N_o with their respective linear velocities at different conditions computed are expressed in Table 4 below. The value of K_{AB} increased with increase in initial concentrations for both PFOA and PFOS, whereas the values decreased with increase in bed loading from 4.2 L min^{-1} mg x 10^{-6} L min^{-1} mg to 3.9 L min^{-1} mg x 10^{-3} L min^{-1} mg and from 9 L min^{-1} mg x 10^{-6} L min^{-1} mg to 8 L min^{-1} mg x 10^{-6} L min^{-1} mg for both PFAS respectively. The flow rate indicated a steady increase in K_{AB} when increased from 0.5 L min^{-1} to 1.5 x 10^{-3} L min^{-1}. The correlation coefficients (R^2) were less than 0.800 in all cases, indicating that experimental data obtained does not conform to this model.

Table 4: Dynamic adsorption parameters for PFOA/PFOS removal by MT pellets – Adam-Bohart model

	K_{TH} (x10^{-3} L min^{-1} mg)		N_o (mg L^{-1})		R^2	
	PFOA	PFOS	PFOA	PFOS	PFOA	PFOS
Bed loading (g)						
0.5	0.0042	0.0009	25	25	0.764	0.603
1	0.0039	0.0008	12.5	12.48	0.711	0.636
1.5	0.0043	0.0012	8.33	8.29	0.643	0.794
Flow rate (x10^{-3} L min^{-1})						
0.5	0.0024	0.0027	4156.91	1197.1	0.238	0.747
1.5	0.0026	0.0026	3061.44	3498.56	0.318	0.754
2.5	0.0025	0.0019	5445.81	6000.8	0.306	0.578
Initial concentration (mg L^{-1})						
5	0.002	0.0023	6888.9	6658.6	0.542	0.736
10	0.0012	0.0009	13690.4	14944.5	0.530	0.563
20	0.0005	00004	31538.4	33179.4	0.473	0.546

Yoon-Nelson model

The linear regression results and correlation coefficient values for this model are presented in Table 5 below. From the table, it can be observed that the rate constant of this model (K_{YN}) and Time (t) required for the adsorbate break through to be at 50% increased and decreased respectively with the increase in the adsorbate dosage. The limited residence time of PFOA and PFOS in adsorbent bed as a result of constant flow rate decreased. The maximum adsorption capacity (qTh) showed a reverse trend for both PFOA and PFOS through all the parameter variations, and this same pattern was reported in a study by [33]. The time required for the adsorbate break through at 50% obtained from

Table 5: Dynamic adsorption parameters for PFOA/PFOS removal by MT pellets - Yoon-Nelson model.

	K_{YN} (L min^{-1})		qTh (mg g^{-1})		R^2	
	PFOA	PFOS	PFOA	PFOS	PFOA	PFOS
Bed loading (g)						
0.5	0.0043	0.682	4472	25	0.776	0.638
1	0.0041	0.605	4474.9	12.447	0.849	0.710
1.5	0.0044	0.808	2763	8.329	0.658	0.827
Flow rate (x10^{-3} L min^{-1})						
0.5	0.0025	0.0028	996.2	1159	0.249	0.763
1.5	0.0027	0.0027	2943.9	6703.9	0.332	0.775
2.5	0.0026	0.0021	5288	5619	0.316	0.609
Initial concentration (mg L^{-1})						
5	0.0023	0.0024	6707	6430	0.554	0.754
10	0.0012	0.0009	13676.9	14582.8	0.538	0.573
20	0.0005	0.0005	31084	32641	0.478	0.554

the Yoon-Nelson model agreed well with the experimental data at most of the conditions examined. Through the values of R^2 it can be concluded that the Thomas model predicts the adsorption performance more satisfactorily than the other two models

CONCLUSION

The performance of MT pellets in the removal of PFOA and PFOS from aqueous matrices was found to be dependent on bed loading, initial concentration and the flow rate of the fixed-bed setup. For instance, it was found that an increase in initial concentration resulted in higher uptakes, noted in change from 5 mg L^{-1} to 10 mg L^{-1}, and ultimately in 20 mg L^{-1} which indicated the highest removal percentage at average bed loading. Additionally, it was noted that an increase in bed height for adsorption had a threshold for highest uptake, since increase from 0.5 g to 1 g showed an increase in removal. However, desorption pattern began to form when bed height increased from 1 g to 1.5 g. Moreover, as the flow rate increased from 0.5 L min^{-1} mg x 10^{-3}L min^{-1} to 1.5 L min^{-1} mg x 10^{-3}L min^{-1}, an increase in K_{TH} values from 7.311 L min^{-1} mg x 10^4 L min^{-1} mg to 7.532 L min^{-1} mg x 10^4 L min^{-1} mg; and 6.831 L min^{-1} mg x 10^4 L min^{-1} mg to 7.722 L min^{-1} mg x 10^4 L min^{-1} mg were observed for PFOA and PFOS respectively. This observation fitted impeccably well to the Thomas model. Moreover, the behaviour of MT pellets for the removal of PFOA and PFOS from surface water indicated that the adsorption was based on a high driving force that was influenced by the increase in initial PFAS concentration. The concentrations of PFOA and PFOS prior to all treatment were calculated at 98 ng mL^{-1} and 125 ng mL^{-1} respectively after the SPE filtration and LCMSMS analysis, and the column study treatment resulted in final concentrations of 29.4 ng mL^{-1} and 31.25 ng mL^{-1} for PFOA and PFOS respectively after removal.

The Adam-Bohart model was the least fitted for the data results of this study. These results indicated that the equations of these two models can be used to predict the adoption behaviour at any operating conditions for the adsorption of PFOA and PFOS onto MT pellets.

REFERENCES

1. Fujii S, Polprasert C, Tanaka S, Lien NPH, Qiu Y. New POPs in the water environment: distribution, bioaccumulation and treatment of perfluorinated compounds–A review paper. J Water Supply Res Technol – Aqua. 2007;56: 313–326.

2. D'eon JC, Crozier PW, Furdui VI, Reiner EJ, Libelo EL, Mabury SA. Perfluorinated phosphonic acids in Canadian surface waters and wastewater treatment plant effluent: discovery of a new class of perfluorinated acids. Environ Toxicol Chem. 2009;28:2101-2107.

3. Busch J, Ahrens L, Sturm R, Ebinghaus R. Polyfluoroalkyl compounds in landfill leachates. Environ Pollut. 2010;158:1467-1471.

4. Liu R, Ruan T, Wang T, Song S, Yu M, Gao Y et al. Trace analysis of mono-, di-, tri-substituted polyfluoroalkyl phosphates and perfluorinated phosphoric acids in sewage sludge by high performance liquid chromatography tandem mass spectrometry. Talanta. 2013;111:170-177.

5. Rao NS, Baker BE. Textile finishes and fluorosurfactants. Plenum. 1994;321-338.

6. Kissa E. Fluorinated surfactants: Synthesis–properties–applications (surfactant science series 50). (1994); Marcel Dekker 469.

7. Kissa E. Fluorinated surfactants and repellents (2nd edition revised and expanded) (Surfactant science series 97). 2001;

Marcel Dekker 640.

8. Taylor CK. Fluorinated surfactants in practice. In: Karsa D, editor. Design and selection of performance surfactants: Annual surfactants review. 1999; John Wiley & Sons 271-316.

9. 3M COMPANY Fluorochemical use, distribution and release overview. USEPA Administrative Record AR226-0550. 1999. Available from: www.regulations.gov as document EPA-HQ-OPPT-2002-0051-0003.

10. Buck RC, Franklin J, Berger U, Conder JM, Cousins IT, de Voogt P et al. Perfluoroalkyl and Polyfluoroalkyl substances in the environment: Terminology, Classiﬁcation, and Origins. Integrated Environ Assess Man. 2011;7 (4): 513-541.

11. UNICEF, WHO meeting the mdg drinking water and sanitation target: a mid-term assessment of progress. UNICEF/WHO, Geneva, Switzerland. 2004.

12. Ning SY, Zou Q, Wang XP, Liu RQ, Wei YZ. Adsorption behavior of Me-2-CA-BTP/SiO2-P adsorbent toward MA (Cravotta and Brady) and Ln (Cravotta and Brady) in nitrate solution. Sci China-Chem. 2016; 59: 862-868.

13. Gasser MS, Elsherif E, Rahman ROA. Modification of Mg-Fe hydrotalcite using Cyanex 272 for lanthanides separation. Chem Eng J. 2017;316: 758-769.

14. Gupta NK, Sengupta A. Understanding the sorption behavior of trivalent lanthanides on amide functionalized multi walled carbon nanotubes. Hydrometallurgy. 2017;171: 8-15.

15. Dorota K, Zbigniew. H Investigation of sorption and separation of lanthanides on the ion exchangers of various types. Ion exchange technologies, UMCS InTech, Int.ed, Poland.

16. Naeem A, Westerhoff P, Mustafa S. Vanadium removal by metal (hydr) oxide adsorbents. water research. 2007;41: 1596-1602.

17. Sekhula Mm, Okonkwo JO, Zvinowanda CM, Agyei NN, Chaudhary AJ. Fixed bed column adsorption of cu (ii) onto maize tassel-pva beads. Journal of Chemistry Engineering Process Technolofy. 2012.

18. Zvinowanda CM. The utilization of maize tassels as an adsorbent for the removal of heavy metals from aqueous solutions. PhD Thesis - Tshwane University of Technology. 2009.

19. Zvinowanda CM, Okonkwo JO, Sekhula MM, Agyei NM, Sadiku R. Application of maize tassel for the removal of Pb, Se, Sr, U and V from borehole water contaminated with mine wastewater in the presence of alkaline metals. J of Haz Mat. 2009a;164(2-3): 884-891.

20. Zvinowanda CM, Okonkwo JO, Sekhula MM, Anyei NM, Sadiku R. Application of maize tassel for the removal of Pb, Se, Sr, U and V from borehole water contaminated with mine wastewater in the presence of alkaline metals. J of haz mat.

2009B;164: 884-891.

21. De Voogt P, Sáez M Analytical chemistry of perfluoroalkylated substances. TrAC Trends in Am Chem. 2006;25: 326-342.

22. Thomas HC. Heterogeneous ion exchange in a flowing system. J A Chem Soc. 1944;66: 1664-1666.

23. Bohart G, Adams EQ. Some aspects of the behaviour of charcoal with respect to chlorine. J Am Chem Soc. 1920;42: 523-544.

24. Yoon TH, Nelson JH. Application of gas adsorption kinetics-II. A theoretical model for respirator cartridge service life and its practical applications. Am Ind Hyg Assoc J. 1984;45: 517-524.

25. Han R, Wang Y, Zou W, Wang Y, Shi J. Comparison of linear and nonlinear analysis in estimating the Thomas model parameters for methylene blue adsorption onto natural zeolite in fixed-bed column. J of Haz Mat. 2007;145 (1-2): 33-336.

26. Han R, Wang Y, Zhao X, Wang Y, Xie F, Cheng J et al. Adsorption of methylene blue by phoenix tree leaf powder in a fixed-bed column: experiments and prediction of break through curves. Desalination. 2009;245: 284-297.

27. Chowdhury ZZ, Zain SM, Rashid AK, Rafique RF, Khalid K. Break through curve analysis for column dynamics sorption of Mn(II) ions from wastewater by using mangotsana garciania peel-based granular activated carbon. J of Chem 2013;95976-959769.

28. Bharrathi KS, Badabhagni N, Nidheesh PV. Break through data analysis of adsorption of cd (ii) on coir pith column. ejeaf Che. 2011;10 (8): 2638-2658.

29. Biswas S, Mishra U. Continuous Fixed-bed column study and adsorption modeling: removal of lead ion from aqueous solution by charcoal originated from chemical carbonization of rubber wood sawdust. J of Chem. 2015;9:3-6.

30. Ahmad AA, Hameed BH. Fixed-bed adsorption of reactive azo dye onto granular activated carbon prepared from waste. J of Haz Mat. 2010;175 (1-3): 298-303.

31. Mittal A, Krishnan L, Gupta VK. Removal and recovery of malachite green from wastewater using an agricultural waste material, de-oiled soya. Separation and Purification Technol. 2005;43: 125-133.

32. Chung WJ, Torrejos REC, Park MJ, Vivas EL, Limjuco LA, Lawagon CP et al. Continuous lithium mining from aqueous resources by an adsorbent filter with a 3D polymeric nanofiber network infused with ion sieves. Chem Eng J. 2017;309: 49-62.

33. Bhaumik M, Setshedi K, Maity A, Onyango MS. Chromium (VI) removal from water using fixed bed column of polypyrrole/Fe3O4 nanocomposite. Sep. Purif. Technol. 2013;110: 11-19.